Monitoring of single-cell bacterial lysis by phages within integrated optical traps

Enrico Tartari, Nicolas Villa, Hugues de Villiers de la Noue, Simon Glicenstein, Emmanuel Picard, Pierre R. Marcoux, Marc Zelsmann, Emmanuel Hadji, Grégory Resch, Romuald Houdré

RESEARCH ARTICLE

ADVANCED OPTICAL MATERIALS
www.advopticalmat.de

Monitoring of Single-Cell Bacterial Lysis by Phages Within Integrated Optical Traps

Enrico Tartari, Nicolas Villa, Hugues de Villiers de la Noue, Simon Glicenstein, Emmanuel Picard, Pierre R. Marcoux, Marc Zelsmann, Emmanuel Hadji, Grégory Resch, and Romuald Houdré*

The bacterial ecosystem is naturally balanced by viruses known as bacteriophages. Accordingly, they represent an emerging adjuvant to antibiotics to fight bacterial infections. However, the interaction of a single bacterium with bacteriophages remains poorly understood. Here, the use of nanoscale light engineering for the fundamental study of single bacterium-phages interaction is demonstrated. The ability to monitor the lysis of single *Escherichia coli* cells challenged by two different types of bacteriophages in silicon-on-insulator photonic crystal (PhC) cavities is shown. These nanostructures allow for the optical trapping of a single phage-infected bacterium and their resonant nature allows deciphering the viability of the bacterium by continuously sensing its interaction with the optical field. L3 and H2 PhC cavities are used for the experiments. While the L3 allows for a fine investigation of the bacterial outer membrane, the H2 allows for the optical trapping of the bacterium even after lysis. The analysis of the post-lysis bacterial response provides information that correlates with phage-specific properties. These results, obtained without any need for preliminary labeling nor bioreceptors, deepen the understanding of the fundamentals of bacteria-phages interaction and pave the way to novel breakthrough tools for phage therapy and more generally for antimicrobial susceptibility testing.

1. Introduction

Bacteriophages, or phages, are viruses that prey on bacteria, and their antagonistic competition is involved in the regulation of most ecosystems on Earth.[1,2] Furthermore, phages have eventually shown their importance as emerging adjuvants to antibiotics for the treatment of difficult-to-treat bacterial infections in a so-called phage therapy approach.[3–7] Therefore, shedding light on the physical interaction of phages with bacteria is crucial for a fundamental understanding of microbial evolution. However, scrutinizing the effect of a 200 nm virus on a 1 µm bacterium with a small footprint and in a non-destructive and label-free approach remains an open challenge. Indeed, current reference techniques,[8] such as drop test, turbidity, and time-kill assays investigate the effects of the interaction at the population level and provide no other information than phage virulence. Despite the efforts to improve

E. Tartari, N. Villa, R. Houdré
Institut de Physique
École Polytechnique Fédérale de Lausanne
Lausanne CH-1015, Switzerland
E-mail: enrico.tartari@epfl.ch

H. de Villiers de la Noue, G. Resch
Laboratory of bacteriophages and phage therapy
CRISP
Lausanne University Hospital (CHUV)
Lausanne 1011, Switzerland

S. Glicenstein, E. Picard, E. Hadji
Univ. Grenoble Alpes
CEA Grenoble
Grenoble INP
IRIG
PHELIQS
SiNaPS
Grenoble 38000, France

P. R. Marcoux
University Grenoble Alpes
CEA
LETI
Minatec-Campus
17 Avenue des Martyrs, Grenoble Cedex 9, 38054, France

M. Zelsmann
University Grenoble Alpes
CNRS
CEA
LETI Minatec
Grenoble INP
LTM
17 Avenue des Martyrs, Grenoble Cedex 9, 38054, France

The ORCID identification number(s) for the author(s) of this article can be found under https://doi.org/10.1002/adom.202402586

DOI: 10.1002/adom.202402586

these classical and empiric techniques, modern approaches, including Polymerase Chain Reaction (PCR),[9] Matrix-Assisted Laser Desorption/Ionization Mass Spectroscopy (MALDI-TOF MS),[10] and flow cytometry,[11] still fail to elucidate the dynamics of bacteria and phages at a fundamental level. Instead, these methods focus on the outcome of the interaction, i.e., the ability of the phage to kill its host, rather than on the dynamic process occurring between the two organisms.

Modern microfabrication technologies and optical engineering at the nanoscale could circumvent the current limitations. Indeed, the light localized within a point-like defect photonic crystal (PhC) cavity possesses rapid field intensity variations which provide an effective integrated optical trap for nanometers to micrometers sized objects.[12–16] Moreover, PhC-based nanotweezers have an optically resonant nature. As a result, the trapped object influences the local field, thereby altering the resonant properties of the cavity.[17–21] This allows to infer information directly related to the trapped object, such as its size or optical properties. So far, PhC nanotweezers allowed for trapping and differentiating bacteria and distinguishing their Gram-type and, very recently, trapping and distinguishing bacteriophages.[22–28] However, their application for real time monitoring of antimicrobial susceptibility has not been shown yet.

Here, we propose a PhC nanotweezer approach for real-time multiparametric monitoring of a single bacterium interacting with phages. This is achieved with a tightly confined optical field that allows probing morphologic and optical modifications of the bacteria without the need for labeling or sensor surface functionalization. In particular, we report the direct detection of single lytic interactions between *Escherichia coli* strain B (*E. coli* B) bacteria and phages T1 or vB_EcoM_1042 (T4) in L3 and H2 PhC cavities. These are specifically designed to be hollow to allow for a maximal overlap of the trapped object with the confined optical field, i.e., the maximum interaction between the field and the specimen. Furthermore, we demonstrate how the H2 cavity can assess the post-lysis state of the bacterium while the L3 is more suited to monitor the eventual bacterial outer membrane degradation upon phage infection. This novel technique not only tests the phage lytic behavior but also shows the ability to infer phage-specific properties and provides information about the dynamics of bacteria and phages interaction. We believe that this approach will provide a fundamental understanding of their antagonistic competition and make a significant contribution to phage therapy as a realistic component to the solution of the antibiotic resistance crisis.

2. Results and Discussion

2.1. Setup and Experimental Protocol to Observe On-Chip Bacterial Lysis

For this work, we developed a homemade optofluidic device (Figure S1a, Supporting Information), combining integrated optics and microfluidics, mounted on an optical bench with an end-fire configuration (Figure S3, Supporting Information), to study phage-bacteria interactions with optical nanotweezers. Briefly, a tunable infrared laser is coupled through optical fibers to the input side of a waveguide of the optofluidic chip and collected from the opposite side. Light is coupled to a PhC cavity through a 1-D defect in the photonic crystal structure that forms a photonic crystal waveguide in a silicon-on-insulator substrate (Figure S1b, Supporting Information).[29] The whole photonic structures are integrated into an SU-8 microfluidic circuit to bring the biological suspensions in proximity of the cavity. The laser wavelength is fixed to match the resonance of the empty cavity and therefore excite its optical mode. The field localized in the cavity generates a force that traps nearby objects by pulling them toward a position with maximum object-field overlap.[30] Thus, the trapping occurs in the near field of the optical cavity. As a result, the presence of the object, its nature, and its residual movement within the trap lead to a direct modification of the resonant frequency of the cavity[20,21,23] and, ultimately, in our setup configuration, to a modification of the collected transmission signal (Figure S2, Supporting Information). This process allows for the real-time acquisition of information linked to the refractive index and morphology of the trapped object.

Two cavities were used to perform the trapping experiments, an H2 hollow cavity and an L3 slotted cavity. They support different optical modes and trapping configurations due to their hollow nature and shape. In the H2 cavity, with its 350 nm radius size, the bacterium can be trapped in a configuration where its longitudinal axis is parallel or perpendicular to the photonic crystal membrane, allowing the cell (≈1.5 µm long and ≈0.55 µm wide, Figure S4, Supporting Information) to fully enter in the hollow cavity. In contrast, in the L3 slotted cavity, whose size is 700 nm long and 160 nm wide, the bacterium can only be trapped with its longitudinal axis parallel to the surface, allowing just the cell wall of the bacterium to be probed. However, the amount of the optical field in the hollow region in the L3 cavity is significantly larger than in the H2 cavity, i.e, a smaller portion of the bacterium can provide a larger resonance detuning.

We designed an experimental protocol that accounts for the interaction kinetics between phages and bacteria, which enables monitoring a trapped and infected bacteria just about to lyse (**Figure 1**). At t0, a sample of 6 mL of a fresh solution composed of 50% (v/v) lysogeny broth (LB), 49.5% (v/v) ultrapure water, and 0.5% (v/v) Triton X-100 was inoculated with 60 µL of an overnight culture of *E. coli* B and incubated at 37 °C (Figure 1a). Of note, Triton X-100 was used at low concentrations to improve the photonic crystal membrane wettability and to prevent bacteria from adhering to the silicon photonic crystal membrane.[24] At t1, previously amplified phages (see *Methods*) were added to the bacterial suspension (Figure 1b). Bacteria and phages were left in contact for several minutes before being injected into the chip at t2 (Figure 1c,d). The scanning electron microscope (SEM) pictures and the supported optical mode for the H2 and L3 cavities computed with the guided mode expansion method[31] in the middle of the silicon slab are presented in Figure 1e,f, respectively. After a few minutes needed by the sample to reach the photonic crystal cavities (t3), the first bacterium gets trapped and the recording starts (Figure 1g).

To adapt the general protocol to the specific bacteria and phages selected (i.e., find the suitable t1 and t2), we performed an in vitro classical turbidity assay in which we challenged *E. coli* B with phage T4 (for phage T1 the results are very similar and thus not shown). According to the growth curve, we confirmed that the 50% (v/v) LB solution containing 0.5% (v/v) Triton

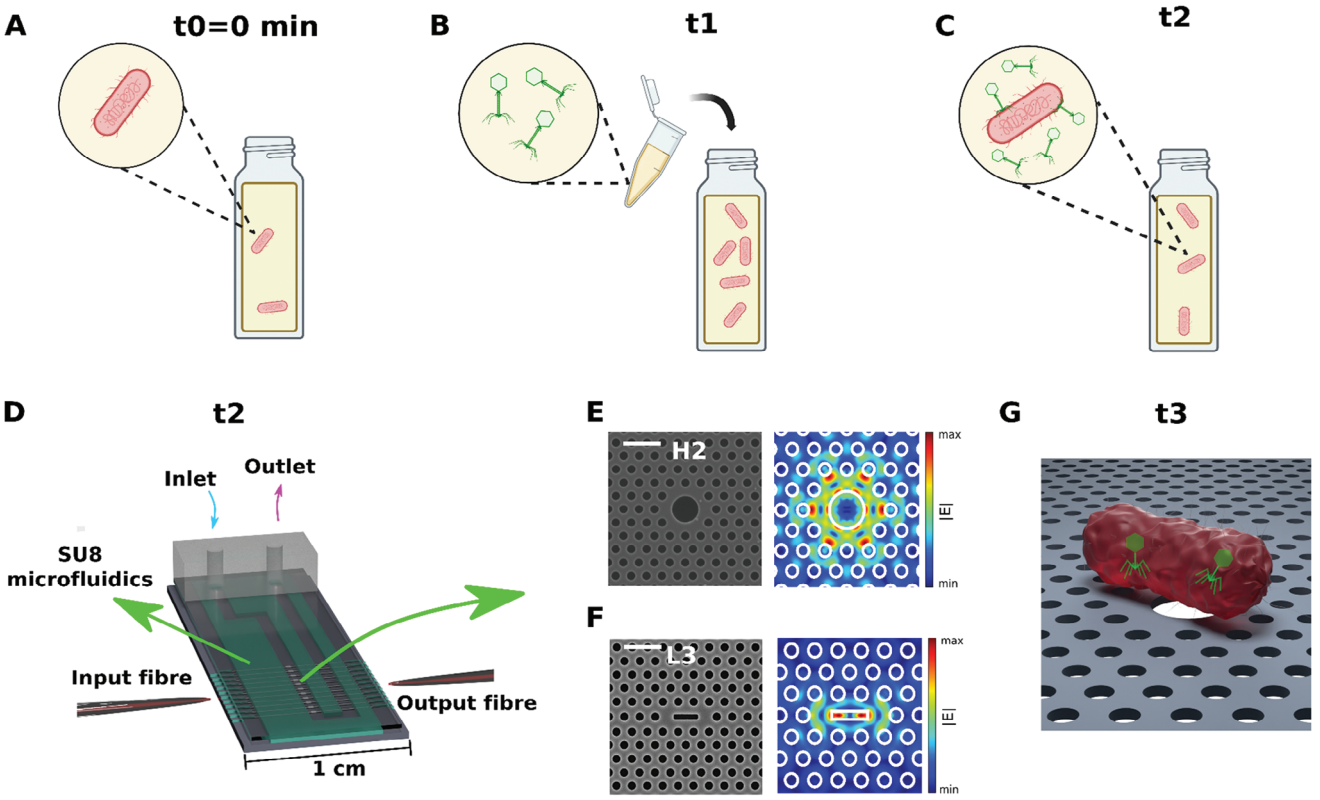

Figure 1. a) The bacterial suspension is incubated at 37 °C at time t0. b) At the exponential phase of growth (time t1), T1 or T4 phages are added to the bacterial suspension at a multiplicity of infection (MOI) of 10. c) At time t2, i.e., after minutes of phages/bacteria co-incubation, an aliquot of the mixture is injected into the optofluidic chip through the inlet. d) Scheme of the assembled optofluidic chip (see Figure S1a, Supporting Information). e,f): Scanning electron micrographs (SEM) of H2 hollow and L3 slot cavities respectively and corresponding optical modes at the center of the slab simulated with the guided mode expansion method. The SEM scale bar is 1 µm. g) Artistic representation of the first single infected bacterium trapped in the H2 hollow cavity at time t3. This corresponds to the start of the trapping experiment.

X-100 had no impact on bacterial growth (**Figure 2**, black curve). The bacterial suspension reached the middle of the exponential growth phase at ≈150 min (t1) after inoculation (t0). At t1, T4 phages were added to the bacterial suspension. At 180 min, i.e., 30 min after the addition of phages, the OD600nm started to drop, in agreement with the time needed for the phages to perform lytic cycles.[32] We expected that injecting the phages bacteria mixture into the optofluidic chip while the curve is decreasing, i.e., when more bacteria are lysing than dividing, would significantly increase the probability of observing a bacterial lysis event on the chip shortly after trapping. Accordingly, we decided to inject 400 µL of the mixture 50 min after the addition of phages (t2 = 200 min). Note that t3, i.e., the time at which the first bacterium gets trapped, is placed on Figure 2 in the middle of the available experimental time slot (i.e., between 200 to 250 min) for the sake of clarity. In the experiments, the first trapping event occurs after 5 ± 2 min from t2.

2.2. Trapping Experiments with the L3 Slotted Cavity

The experiment consisted in trapping a single phage-infected bacterium long enough to record and detect any significant variations in the normalized transmission signal that would reflect lysis following phage infection. We ensured that only one cell was trapped at a time thanks to the experimental imaging system (Figure S3 and Video S4, Supporting Information). In the main text, a single representative measurement per cavity-phage combination is shown for clarity, while more measurements supporting the analysis and interpretation of the results are available in the Supporting Information.

In **Figure 3a** we report a representative control measurement in which a single bacterium originating from a sample taken from a phage-devoid bacterial suspension was trapped in the L3 slot cavity.

We observe that the normalized transmission signal is constant at ≈1.62 ± 0.06 over the entire trapping period. This suggests that the bacterium state remains constant in the trap over the trapping time. The average normalized transmission value for the full set of control measurements is 1.55 ± 0.13 (Figure S5a-i, Supporting Information). In Figure 3b we show a representative experiment measurement in which a single bacterium originating from a sample taken from a T4 -phage/bacteria mixture was trapped in the L3 cavity. In addition, videos were recorded from the imaging system in parallel to the transmission signal, providing visual support for the bacterial morphological changes during the trapping period (Supplementary videos). Representative frames with contrast optimized for clarity are presented in

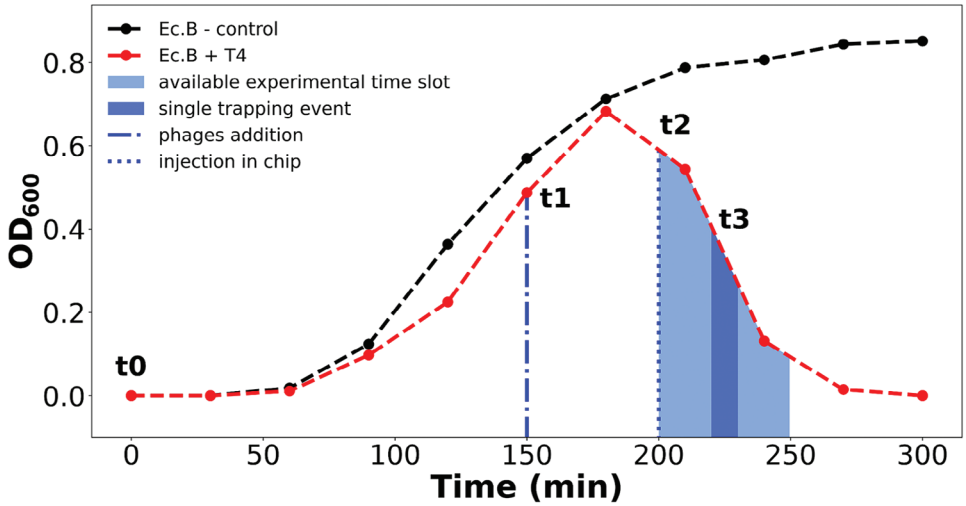

Figure 2. Turbidity assay. Control, i.e., *E. coli* B in LB broth 50%, DI water 49.5%, and Triton X-100 0.5% (v/v) (black curve). *E. coli* B in LB broth 50%, DI water 49.5%, and Triton X-100 0.5% (v/v) challenged with T4 phage (red curve). The bacterial suspension was incubated at 37 °C at t0 = 0 min. During the exponential phase of growth, at t1 = 150 min, T4 phages were added to the bacterial suspension at a MOI of 10. After 50 min of phages/bacteria co-incubation 400 µL of the mixture was injected into the optofluidic chip through the inlet (t2 = 200 min) and the trapping measurements started at t3.

Figure 3c. The normalized signal remains constant for ≈50 s at 1.45 ± 0.03 (Figure 3b-1), indicating no occurring modification of the bacterial cell as confirmed by the video recording (Figure 3c, frame 1; Video S1, Supporting Information). Interestingly, the normalized signal then gradually decreases between 100 s and 250 s to 1.21±0.03 (Figure 3b-2), before stabilizing at this level for 50 s (Figure 3b-3). One explanation of this time evolution could be the effect of the phage-encoded holin-endolysin system. While holins are inner membrane pore-forming proteins, endolysins diffuse through the holin pores. Once in the periplasmic space, endolysins induce bacterial burst by cell wall peptidoglycan hydrolysis for phage progeny release from the bacterial cytoplasm.[33] Physically, the holin-endolysin system activity causes a dramatic increase in the bacterium's osmotic pressure due to the permeabilization of the bacterial cell wall. Liquid influxes in the cell's cytoplasm have two major consequences. First, they contribute to lowering the cell's refractive index, and second, they induce morphological variations, notably by swelling the bacterium (see Figure 3c, frames 2 and 3, respectively, and Video S1, Supporting Information). These effects directly impact the overlap of the bacterium with the optical field and the refractive index contrast between the bacterium and the environment, dictating how the cavity mode is perturbed and ultimately influencing the transmitted power through the chip. Therefore, the reduction of the refractive index contrast lowers the normalized signal, and the bacterium swelling enlarges the cell, likely making it less deformable. Thus, it prevents the bacterium from entering the hollow region of the cavity where the light-matter interaction is the greatest. This observation is in agreement with previous works where PhC cavities were used to distinguish between the Gram types of selected bacterial species, which depends on the properties of the cell wall.[23] This suggests that the optical cavity can resolve cell wall properties of the trapped bacterium and hence provide an indication of its state, which, in this experiment, is likely to be significantly impacted by the activity of the holin-endolysin system. At 300 s, we then observed an abrupt drop of the signal to 1.00 ± 0.01, which is the signature of an empty trap (Figure 3b-3, black dotted line). The signal stabilizes at this value for the remaining experimental time (Figure 3b-4). The event of bacterial lysis by phages corresponds to this sharp drop in the transmission signal. Indeed, the important alteration of the bacterial morphology resulting from the cell burst to release the virion progeny is expected to induce a strong decrease in the optomechanical coupling between the destroyed bacterium and the resonant mode due to a significantly reduced overlap between the object and the localized field in the cavity and finally the release of the bacterial debris from the cavity. This scenario is perfectly supported by the visual recording in which a clear cell burst is visualized at the time of the signal drop (Figure 3c, frame lysis; Video S1, Supporting Information), followed by the visualization of an empty cavity until the end of the recording (Figure 3c, frame 4; Video S1, Supporting Information). The signal presented corresponds, to the best of our knowledge, to the first direct observation of a lytic interaction at the level of a single bacterium trapped in a photonic crystal cavity.

2.3. Trapping Experiments with the H2 Hollow Cavity

We repeated the same protocol described in Figure 1 with *E. coli B* and T4, this time using an H2 hollow cavity. In **Figure** 4a we see a representative control measurement where a single bacterium from a phage-devoid bacterial suspension in the exponential phase was trapped in the H2 cavity. We observe that the normalized transmission signal is constant at ≈1.95 ± 0.07 over the entire trapping period (the average normalized transmission value for the full set of control measurements being 1.82 ± 0.13, Figure S5j–r, Supporting Information). This indicates, as in the case of the L3 cavity, that the state of the bacterium remains constant in the trap over the trapping time.

In Figure 4b, we report a representative experiment measurement in which a single bacterium originating from a

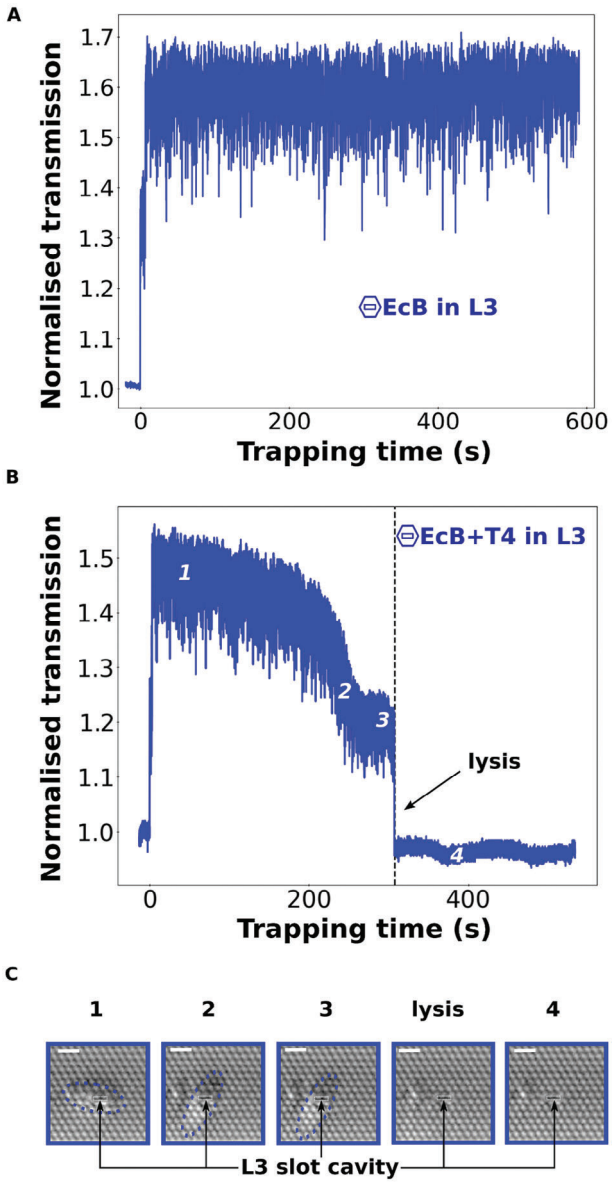

Figure 3. a) Control trace of a selected *E. coli* B cell being trapped in an L3 slot cavity. No bacteriophages are present in the suspension. b) Lysis trace of a selected *E. coli* B cell infected by T4 bacteriophages being trapped in an L3 slot cavity. The lysis corresponds to the abrupt decrease of transmission at ≈300 s of trapping time. The return to the transmission value of an empty cavity means that the trap was empty right after the lysis. c) Selected frames of the time-lapse acquired through the imaging camera (see Video S1, Supporting Information for the full time-lapse). The L3 slot cavity is highlighted in all the frames by a white dotted rectangle, and blue dotted ellipses depict the bacterium in frames 1–3. In each frame, the white scale bar represents 1 µm.

T4-phage/bacteria mixture was trapped in the H2 cavity. Similarly to Figure 3b, we observe a slow decrease from 1.95 ± 0.06 to 1.78 ± 0.07 of the transmission signal for the first 100 s (see Figure 4b-1,b-2). Then, an abrupt drop from 1.78 ± 0.07 to 1.0 ± 0.01 occurs at the lysis time. However, an important qualitative difference with respect to the L3 cavity is the higher overlap between the cell and the optical mode of the H2 hollow cavity. This grants the small opto-mechanical coupling between the lysed bacterium and the cavity mode to be strong enough to keep the lysed corpse trapped, even if for 10 s after the lysis in this case (see Figure 4b-3). This means that, using H2 cavities, real-time information can be retrieved for the trapped bacterium before, during, and after lysis. Accordingly, the H2 cavity appears most suited for on-chip lysis investigation as the final morphology of the bacterium could provide interesting information about the phage virulence and burst size.

To test this hypothesis, we selected the H2 cavity to perform the next experiment. The goal was to compare the virulence of two different phages (T4 and T1) on the same host. In Figure 4d, we report a representative measurement in which a single bacterium originating from a T1-phage/bacteria mixture was trapped in the H2 cavity. First of all, we observe that there is no slow decrease of the signal before lysis as observed for T4. From the full set of measurements (Figures S6 and S7, Supporting Information) it emerges that the slow decrease of the signal was more probably observed for the T4-infected bacteria than the T1-infected ones (60% and 40% of the measurements for T4 and T1, respectively, in L3, while 40% and 20% of the measurements for T4 and T1, respectively, in H2). This could indicate a different endolytic effect of the T1 phage compared to the T4 phage. Moreover, the L3 cavity harbors higher sensitivity in addressing phages' holin-endolysin system, likely involved in the slow decrease in the transmission signal before lysis. Indeed, this observation corroborates the fact that the L3 geometry and optical mode are more suited to investigate the degradation of the outer membrane of the bacteria. For the T1-infected bacterium trapped in the H2 cavity, the signal remains constant at 1.75 ± 0.06 for the first 350 s (Figure 4d-1,d-2). Finally, the lysis corresponds to the drop after 375 s pointed by the arrow, before the transmission signal increases back to 1.47 ± 0.07. We confirmed that the nature of the H2 cavity allows for the trapping of the lysed bacteria even in the case of the lysis by a T1 phage. We remark that trapping a lysed bacterium infected by T1 phages for more than 20 s was more probable than for a T4-lysed bacterium (60% for T1-lysed and 0% for T4-lysed bacteria over 10 measurements each, Figures S6 and S7, Supporting Information). Indeed, comparing Figure 4b,d, we observe that the trapping of a T4 lysed bacterium was possible just for a few seconds while the T1 lysed one could be trapped for more than 50 s (see Figure 4d-4). Moreover, for the T1-infected bacterium, the signal recovered a value of 1.47 ± 0.07, i.e., 84% of the pre-lysis signal, likely indicating a less intense burst compared to the T4 case. To investigate if the difference correlated with phage-specific properties, the burst sizes and latent periods of T4 and T1 phages were determined on *E. coli* B from the analysis of classical one-step growth curves (**Table 1**), see Experimental Section and Figure S8 (Supporting Information). While latent periods were similar (13 ± 1 vs 19 ± 1 min), T4 phage infection of *E. coli* B resulted in twice higher average burst size than for T1 infection (149 ± 1.8 vs 74 ± 3, respectively). These burst size differences correlate well with the ability or difficulty of trapping the bacterial corpse or its fragments after the lytic event caused by the two phages. In fact, releasing twice as many phages following T4 lysis could damage the bacterium to a greater extent than a T1 lysis, leading to the inability to trap the corpse of such a heavily T4-damaged bacterium.

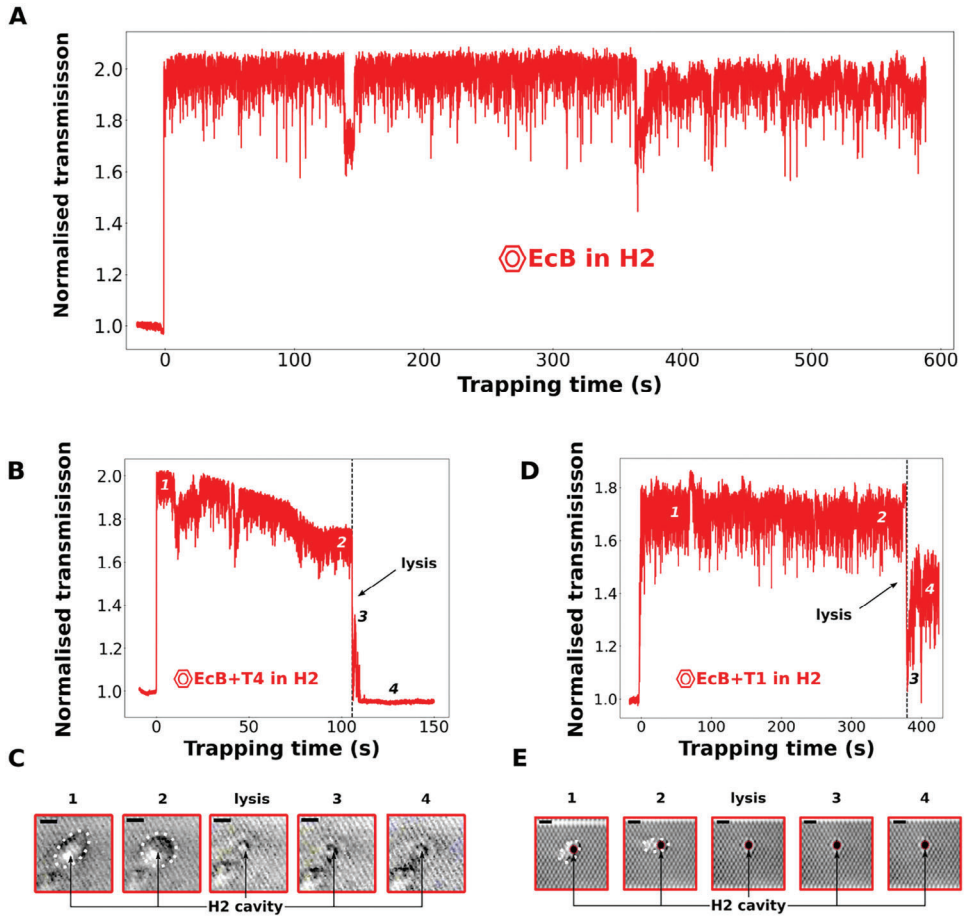

Figure 4. a) Control trace of a selected *E. coli* B cell being trapped in an H2 hollow cavity. No bacteriophages are present in the suspension. b) Lysis trace of a selected *E. coli* B cell infected by T4 bacteriophages being trapped in an H2 hollow cavity. The lysis corresponds to the abrupt decrease of transmission at ≈110 s of trapping time. The signal perturbation after the lysis remains present for only a few seconds, meaning that the corpse of the bacterium could be trapped, but not stably. c) Selected frames of the time-lapse acquired through the imaging camera for the lytic trace of panel b (see Video S2, Supporting Information for the full time-lapse). The H2 hollow cavity is indicated by arrows, and white dotted ellipses depict the bacterium in frames 1–2. In each frame, the scale bar represents 1 µm. d) Lysis trace of a selected *E. coli* B cell infected by T1 bacteriophages being trapped in an H2 hollow cavity. The lysis corresponds to the abrupt decrease of transmission at ≈385 s. In this case, the corpse of the bacterium can still be trapped after the lysis, providing a stable normalized transmission larger than the transmission of an empty cavity. e) Selected frames of the time-lapse acquired through the imaging camera for the lytic trace of panel d) (see Video S3, Supporting Information for the full time-lapse). The H2 hollow cavity is highlighted in all the frames by a white dotted circle, and red dotted ellipses depict the bacterium in frames 1–2. In each frame, the black scale bar represents 1 µm.

3. Conclusion

We showed how the nanoscale engineering of light can be used to perform real-time multiparametric monitoring of a single bacterium interacting with phages. We demonstrate, for the first time to our knowledge, the direct observation of single bacterium – bacteriophages lytic interactions in a photonic crystal cavity. In particular, the lysis of single *E. coli* B cells challenged by two different bacteriophages (T1, T4) was explored. The optical cavities allow for the optical trapping of a single phage-infected bacterium, while their resonant nature allows for probing any morphologic and optical modifications with single-cell sensitivity. Two cavities were used for the experiments, L3 and H2 cavities. Due to their different geometry and distinct optical modes they are suited for probing different properties. The former allows for a fine investigation of the outer membrane of the bacterium while the latter allows to keep the bacterium optically trapped after the lysis. The analysis of the post-lysis bacterial response provides information that showed correlations to phage species-specific properties such as the burst size. Our approach relies on optical forces to immobilize objects, thus eliminating the need for bioreceptors or staining. In addition, resonant cavities not only

Table 1. Measured burst size and latent period for T4 and T1 bacteriophages on *E. coli* B measured by one-step growth assays.

Bacteriophage	Latent period [min]	Burst size [PFU]	Probability to trap lysed bacterium for t > 20 s in H2 cavity [$n = 10$]
T4	13 ± 1	149 ± 1.8	0%
T1	19 ± 1	74 ± 3	60%

detect lysis but also provide real-time information about the interaction. The experiment is suited to be multiplexed using tens of cavities, excited using fiber arrays and splitting waveguides to perform multiple single-cell trapping measurements simultaneously. Working at the single-cell level allows us to assess the variability of phage's infection over the bacterial population. In particular, in future developments, we envision monitoring bacteria's responses before, during and after phage's infection, opening the way to more information about processes occurring during bacteria-phages interaction.

Currently, several challenges remain to be solved before phage therapy could be used routinely at the clinic. Due to the strong phage infecting specificity, phage cocktails covering many different bacterial isolates were sometimes preferred (one-drug-fits-all approach).[5,34] However, developing such cocktails is not realistic for many bacterial species, again because of the strain-specificity of phages as demonstrated by recent clinical trials.[35–39] Accordingly, the scientific community tends to agree that phage therapy should be personalized to the strain infecting the patient (tailored approach).[40] In turn, it becomes necessary to screen large collections of phages to select the most suited ones, and this remains a main obstacle to the development of personalized phage therapy clinical trials.

We believe that this novel approach to perform a multiparametric label-free bacteria-phages interaction analysis at the single-cell level using the sheer properties of light can help in such a challenge and lead to innovative breakthroughs in the field of antimicrobial susceptibility tests. At the same time, it could represent an important contribution to the consolidation of phage therapy and a crucial step forward in the fight against bacterial infections whose cure is extremely hard due to antimicrobial resistance.[41–45]

4. Experimental Section

Optofluidic Device Fabrication: The photonic crystal cavities are prepared via electron beam lithography patterning of ZEP resist, followed by the transfer onto a 220 nm silicon layer through inductively coupled plasma etching. Two photolithography steps are performed to pattern the SU-8 mode converters, and SU-8 microfluidic channels, 750 µm wide and 25 µm thick. The facets are cleaved allowing for near-infrared laser light coupling with the input and output fibers. The photonic crystal membranes are suspended using wet buffered HF etching to ensure optimal vertical confinement of the optical mode. Finally, a 145 µm glass coverslip suitable for immersion oil microscopy is placed to seal the fluidic system. Biological suspensions are injected into the chip microchannels via an inlet tube inserted into a polydimethylsiloxane (PDMS) interconnect, and extracted from the outlet and transferred to the waste.

Bacteria Strain, Phages and Phages Amplification: As biological samples, *E. coli* B were selected from our own collection. For the bacteriophages, T1 and T4 phages were used from Centre Hospitalier Universitaire Vaudois (CHUV). Bacteria were grown on Luria Bertani agar Petri dishes at 37 °C overnight for the trapping experiments. Phage T4, phage T1 amplification is performed in Lysogeny broth (LB) with the same *E. coli* B and the phage amplified suspension is then filtered at 0.45 µm with a polyethersulfone filter to remove bacterial residues. Characterization of phages concentration after the amplification by drop dilution test resulted in 10^8–10^9 PFU mL^{-1} suspensions.

One-Step Growth Assays: One-step growth assays were performed at CHUV. The protocol was based on the one provided by Andrew M. Kropinski.[45] Briefly, *E. coli B* cells were grown from an overnight culture in 25 mL liquid LB (Difco LB Broth Miller, BD Biosciences, 244 620) + 2 mM $CaCl_2$ (Honeywell, 21 114) until reaching mid-log phase (ca. 0.5 OD_{600nm}). 9.9 mL of the log phase culture was then placed into an empty flask (adsorption flask) at 37 °C for 5 min, and 100 µL of phage solution at 10^6 PFU mL^{-1} was added. The flask was incubated for 5 min again at 37 °C, then 100 µL was removed and added to Flask A containing 9.9 mL LB. After mixing, 1 mL of flask A was immediately added to 50 µL $CHCl_3$ (Sigma–Aldrich, C2432) and kept on ice. At the same time, 1 mL of flask A was added to flask B containing 9 mL of LB, mixed, and then 1 mL of flask B was added to flask C containing 9 mL of LB. The three flasks were incubated at 37 °C. Every 5 to 10 min, 100 µL were removed from flasks A, B, and C, added to 4 mL soft LB medium (composed of Difco LB Broth Miller (BD Biosciences, 244 620), Difco agar Bacteriological (BD Biosciences, 214 530) and pure water) together with 100 µL of the *E. coli B* log phase culture. This step was done in triplicates. At the end of the sampling, (ca. 1h), 100 µL of the $CHCl_3$/flask A mix was plated using the same protocol. Overlays were left to harden, and incubated overnight at 37 °C. Lysis plaques were then counted for each time point, and growth curves were traced using GraphPad Prism software (version 10.1.2) and presented in Figure S8 (Supporting Information).

Supporting Information

Supporting Information is available from the Wiley Online Library or from the author.

Acknowledgements

E.T., N.V., H.D.N., E.H., G.R., and R.H. contributed equally to this work. E.T., N.V., and H.D.N. should be considered the first authors. E.H., G.R., and R.H. should be considered the last authors. This work was supported by the Swiss National Science Foundation (SNSF) through grants (nos. 310030L_212772 and 200020_188649), the French RENATECH network and by the French National Research Agency (ANR) through the SUPPLY project (grant no. ANR-22-CE93-0011-01).

Conflict of Interest

The authors declare no conflict of interest.

Data Availability Statement

The data that support the findings of this study are available from the corresponding author upon reasonable request.

Keywords

bacteriophages-bacteria lysis, light nano-engineering, optical trapping, photonic crystals, single-cell

Received: September 24, 2024
Revised: November 18, 2024
Published online: January 25, 2025

[1] Z. Naureen, A. Dautaj, K. Anpilogov, G. Camilleri, K. Dhuli, B. Tanzi, P. E. Maltese, F. Cristofoli, L. D. Antoni, T. Beccari, M. Dundar, M. Bertelli, *Acta Biomed. Atenei Parm.* **2020**, *91*, 2020024.
[2] M. R. J. Clokie, A. D. Millard, A. V. Letarov, S. Heaphy, *Bacteriophage* **2011**, *1*, 31.

[3] F. L. Gordillo Altamirano, J. J. Barr, *Clin. Microbiol. Rev.* **2019**, *32*, 00066.
[4] J. N. Housby, N. H. Mann, *Drug Discov. Today* **2009**, *14*, 536.
[5] B. K. Chan, S. T. Abedon, C. Loc-Carrillo, *Future Microbiol.* **2013**, *8*, 769.
[6] C. Loc-Carrillo, S. T. Abedon, *Bacteriophage* **2011**, *1*, 111.
[7] J.-P. Pirnay, T. Ferry, G. Resch, *FEMS Microbiol. Rev.* **2022**, *46*, fuab040.
[8] V. Daubie, H. Chalhoub, B. Blasdel, H. Dahma, M. Merabishvili, T. Glonti, N. De Vos, J. Quintens, J.-P. Pirnay, M. Hallin, O. Vandenberg, *Front. Cell. Infect. Microbiol.* **2022**, *12*, 1000721.
[9] H. Liu, Y. D. Niu, J. Li, K. Stanford, T. A. McAllister, *Biomed Res. Int.* **2014**, *2014*, 319351.
[10] J. C. Rees, J. R. Barr, *Anal. Bioanal. Chem.* **2017**, *409*, 1379.
[11] L. D. R. Melo, R. Monteiro, D. P. Pires, J. Azeredo, *Antibiotics* **2022**, *11*, 164.
[12] C. Pin, J.-B. Jager, M. Tardif, E. Picard, E. Hadji, F. De Fornel, B. Cluzel, *Lab Chip* **2018**, *18*, 1750.
[13] C. Renaut, J. Dellinger, B. Cluzel, T. Honegger, D. Peyrade, E. Picard, F. De Fornel, E. Hadji, *Appl. Phys. Lett.* **2012**, *100*, 101103.
[14] C. Renaut, B. Cluzel, J. Dellinger, L. Lalouat, E. Picard, D. Peyrade, E. Hadji, F. De Fornel, *Sci. Rep.* **2013**, *3*, 2290.
[15] Y.-F. Chen, X. Serey, R. Sarkar, P. Chen, D. Erickson, *Nano Lett.* **2012**, *12*, 1633.
[16] P. Kang, X. Serey, Y.-F. Chen, D. Erickson, *Nano Lett.* **2012**, *12*, 6400.
[17] J. Hu, S. Lin, L. C. Kimerling, K. Crozier, *Phys. Rev. A* **2010**, *82*, 053819.
[18] M. L. Juan, R. Gordon, Y. Pang, F. Eftekhari, R. Quidant, *Nat. Phys.* **2009**, *5*, 915.
[19] N. Descharmes, U. P. Dharanipathy, Z. Diao, M. Tonin, R. Houdré, *Lab Chip* **2013**, *13*, 3268.
[20] L. Lalouat, B. Cluzel, P. Velha, E. Picard, D. Peyrade, J. P. Hugonin, P. Lalanne, E. Hadji, F. De Fornel, *Phys. Rev. B* **2007**, *76*, 041102.
[21] B. Cluzell, L. Lalouat, P. Velha, E. Picard, D. Peyrade, J.-C. Rodier, T. Charvolin, P. Lalanne, F. De Fornel, E. Hadji, *Opt. Express* **2008**, *16*, 279.
[22] P. Jing, J. Wu, G. W. Liu, E. G. Keeler, S. H. Pun, L. Y. Lin, *Sci. Rep.* **2016**, *6*, 19924.
[23] R. Therisod, M. Tardif, P. R. Marcoux, E. Picard, J.-B. Jager, E. Hadji, D. Peyrade, R. Houdré, *Appl. Phys. Lett.* **2018**, *113*, 111101.
[24] N. Villa, E. Tartari, S. Glicenstein, H. de Villiers de la Noue, E. Picard, P. R. Marcoux, M. Zelsmann, G. Resch, E. Hadji, R. Houdré, *Small* **2024**, *20*, 2308814.
[25] M. Tardif, J.-B. Jager, P. R. Marcoux, K. Uchiyamada, E. Picard, E. Hadji, D. Peyrade, *Appl. Phys. Lett.* **2016**, *109*, 133510.
[26] M. Tardif, E. Picard, V. Gaude, J.-B. Jager, D. Peyrade, E. Hadji, P. R. Marcoux, *Small* **2022**, *18*, 2103765.
[27] T. van Leest, J. Caro, *Lab Chip* **2013**, *13*, 4358.
[28] P. Kang, P. Schein, X. Serey, D. O'Dell, D. Erickson, *Sci. Rep.* **2015**, *5*, 12087.
[29] H. Taniyama, *J. Appl. Phys.* **2002**, *91*, 3511.
[30] A. Ashkin, J. M. Dziedzic, *Berichte Bunsenges. Für Phys. Chem.* **1989**, *93*, 254.
[31] M. Minkov, I. A. D. Williamson, L. C. Andreani, D. Gerace, B. Lou, A. Y. Song, T. W. Hughes, S. Fan, *ACS Photonics* **2020**, *7*, 1729.
[32] S. T. Abedon, T. D. Herschler, D. Stopar, *Appl. Environ. Microbiol.* **2001**, *67*, 4233.
[33] M. Schmelcher, D. M. Donovan, M. J. Loessner, *Future Microbiol.* **2012**, *7*, 1147.
[34] B. K. Chan, S. T. Abedon, *Adv. Appl. Microbiol.* **2012**, *78*, 22305091.
[35] P. Jault, T. Leclerc, S. Jennes, J. P. Pirnay, Y.-A. Que, G. Resch, A. F. Rousseau, F. Ravat, H. Carsin, R. L. Floch, J. V. Schaal, C. Soler, C. Fevre, I. Arnaud, L. Bretaudeau, J. Gabard, *Lancet Infect. Dis.* **2019**, *19*, 35.
[36] S. A. Sarker, S. Sultana, G. Reuteler, D. Moine, P. Descombes, F. Charton, G. Bourdin, S. McCallin, C. Ngom-Bru, T. Neville, M. Akter, S. Huq, F. Qadri, K. Talukdar, M. Kassam, M. Delley, C. Loiseau, Y. Deng, S. El Aidy, B. Berger, H. Brüssow, *EBioMedicine* **2016**, *4*, 124.
[37] R. S. Breederveld, *Lancet Infect. Dis.* **2019**, *19*, 2.
[38] J.-P. Pirnay, E. Kutter, *Lancet Infect. Dis.* **2021**, *21*, 309.
[39] L. Leitner, A. Ujmajuridze, N. Chanishvili, M. Goderdzishvili, I. Chkonia, S. Rigvava, A. Chkhotua, G. Changashvili, S. McCallin, M. P. Schneider, M. D. Liechti, U. Mehnert, L. M. Bachmann, W. Sybesma, T. M. Kessler, *Lancet Infect. Dis.* **2021**, *21*, 427.
[40] B. Zalewska-Piątek, *Pharmaceuticals* **2023**, *16*, 1638.
[41] K. Lewis, *Cell* **2020**, *181*, 29.
[42] E. Tacconelli, E. Carrara, A. Savoldi, S. Harbarth, M. Mendelson, D. L. Monnet, C. Pulcini, G. Kahlmeter, J. Kluytmans, Y. Carmeli, M. Ouellette, K. Outterson, J. Patel, M. Cavaleri, E. M. Cox, C. R. Houchens, M. L. Grayson, P. Hansen, N. Singh, U. Theuretzbacher, N. Magrini, A. O. Aboderin, S. S. Al-Abri, N. Awang Jalil, N. Benzonana, S. Bhattacharya, A. J. Brink, F. R. Burkert, O. Cars, G. Cornaglia, et al., *Lancet Infect. Dis.* **2018**, *18*, 318.
[43] C. L. Ventola, *P T Peer-Rev. J. Formul. Manag.* **2015**, *40*, 277.
[44] B. Aslam, W. Wang, M. I. Arshad, M. Khurshid, S. Muzammil, M. H. Rasool, M. A. Nisar, R. F. Alvi, M. A. Aslam, M. U. Qamar, M. K. F. Salamat, Z. Baloch, *Infect. Drug Resist.* **2018**, *11*, 1645.
[45] A. M. Kropinski, in *Bacteriophages* (Eds: M.R.J. Clokie, A.M. Kropinski, R. Lavigne), Springer, Berlin, New York **2018**, pp. 41–47.